iScience

CellPress
OPEN ACCESS

Article

Implementation of dietary methionine restriction using casein after selective, oxidative deletion of methionine

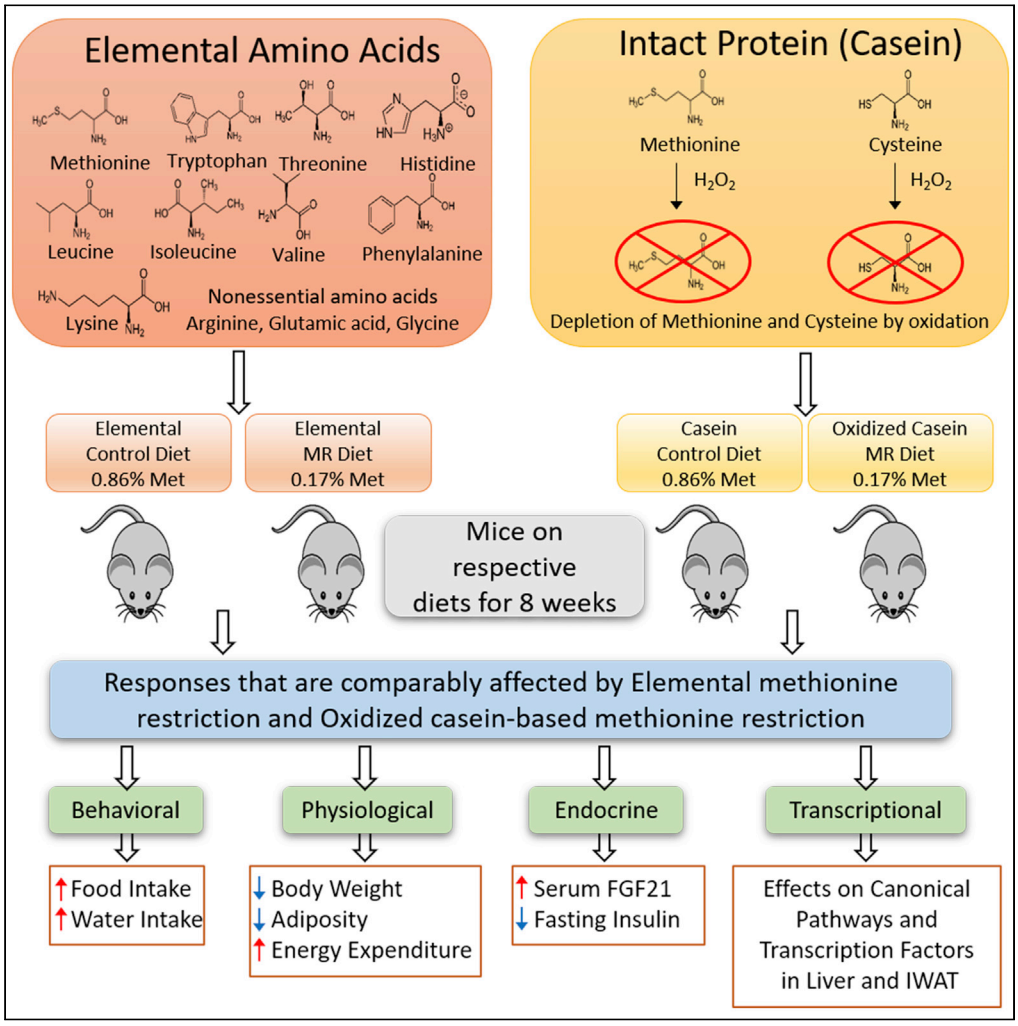

Han Fang, Kirsten P. Stone, Laura A. Forney, Landon C. Sims, Gabriela C. Gutierrez, Sujoy Ghosh, Thomas W. Gettys

thomas.gettys@pbrc.edu

Highlights

Dietary methionine restriction improves biomarkers of metabolic health.

Elemental amino acid-based diets to restrict methionine are highly unpalatable.

Methionine has been depleted from casein by mild oxidation to solve low palatability.

Methionine restriction with oxidized casein is equally effective as elemental diet.

Fang et al., iScience 24, 102470
May 21, 2021
https://doi.org/10.1016/j.isci.2021.102470

iScience

CellPress
OPEN ACCESS

Article

Implementation of dietary methionine restriction using casein after selective, oxidative deletion of methionine

Han Fang,[1] Kirsten P. Stone,[1] Laura A. Forney,[1,2] Landon C. Sims,[1] Gabriela C. Gutierrez,[3] Sujoy Ghosh,[4,5] and Thomas W. Gettys[1,6,*]

SUMMARY

Dietary methionine restriction (MR) is normally implemented using diets formulated from elemental amino acids (AA) that reduce methionine content to ~0.17%. However, translational implementation of MR with elemental AA-based diets is intractable due to poor palatability. To solve this problem and restrict methionine using intact proteins, casein was subjected to mild oxidation to selectively reduce methionine. Diets were then formulated using oxidized casein, adding back methionine to produce a final concentration of 0.17%. The biological efficacy of dietary MR using the oxidized casein (Ox Cas) diet was compared with the standard elemental MR diet in terms of the behavioral, metabolic, endocrine, and transcriptional responses to the four diets. The Ox Cas MR diet faithfully reproduced the expected physiological, biochemical, and transcriptional responses in liver and inguinal white adipose tissue. Collectively, these findings demonstrate that dietary MR can be effectively implemented using casein after selective oxidative reduction of methionine.

INTRODUCTION

The biological responses to restriction of dietary methionine have been the subject of intense interest since the life extending properties of this dietary regimen were originally reported (Orentreich et al.; Richie et al.). Dietary methionine restriction (MR) is implemented by formulating an elemental amino-acid-based semi-purified diet that reduces methionine content by ~80% and eliminates dietary cysteine. The original description of the MR diet by Orentreich and colleagues (Orentreich et al., 1993; Richie et al., 1994) documented its ability to increase mean and maximal life span in rats. Their findings have since been extended to other species (Richie et al., 1994), and in contrast to caloric restriction, the life extending properties of the MR diet do not require food restriction (Malloy et al., 2006; Orentreich et al., 1993; Richie et al., 1994). The short-term physiological responses to dietary MR have received far more attention in the last decade because the diet also extends healthspan by producing immediate and lasting improvements in essentially all biomarkers of metabolic health (Ghosh et al., 2017; Hasek et al., 2010; Lee et al., 2014; Lees et al., 2014; Malloy et al., 2006, 2013; Miller et al., 2005; Perrone et al., 2008, 2009, 2012a, 2012b; Plaisance et al., 2010; Sun et al., 2009; Wanders et al., 2014; Zimmerman et al., 2003). An important advance in understanding how dietary MR produces this beneficial metabolic phenotype came with the recognition that hepatic sensing of reduced methionine activated a series of transcriptional programs in the liver (Ghosh et al., 2014; Hasek et al., 2010; Jonsson et al., 2021; Lees et al., 2014; Perrone et al., 2012b; Stone et al., 2014; Wanders et al., 2014, 2017). Loss-of-function studies showed that hepatic fibroblast growth factor 21 (FGF21) was a key component of this integrated stress response (ISR) and responsible for the ability of the MR diet to increase energy expenditure (EE), reduce fat deposition, and remodel white adipose tissue (Wanders et al., 2017). Dietary MR also reduces the capacity of the liver to synthesize and export fat through transcriptional mechanisms that appear independent of FGF21 (Hasek et al., 2013; Wanders et al., 2017). Collectively, these responses improve the metabolic health of the animal in the days and weeks following introduction of the MR diet (Hasek et al., 2010; Lees et al., 2014).

Given the enormous impact of metabolic disease on the nation's health, the translational potential of a dietary approach that is effective in mitigating all the major components of metabolic disease is

[1]Laboratory of Nutrient Sensing and Adipocyte Signaling, Pennington Biomedical Research Center, Baton Rouge, LA 70808, USA

[2]Department of Integrative Biology and Pharmacology, University of Texas Health Science Center at Houston, Houston, TX 77030, USA

[3]School of Nutrition and Food Sciences, Louisiana State University, Baton Rouge, LA 70809, USA

[4]Laboratory of Computational Biology, Pennington Biomedical Research Center, Baton Rouge, LA 70808, USA

[5]Program in Cardiovascular and Metabolic Disorders and Centre for Computational Biology, Duke-NUS Medical School, Singapore, Singapore

[6]Lead contact

*Correspondence: thomas.gettys@pbrc.edu

https://doi.org/10.1016/j.isci.2021.102470

Table 1. Composition of the control and elemental methionine-restricted diets[a]

Ingredient	Concentration in control diet (g/kg diet)	Concentration in MR diet (g/kg diet)
L-arginine	11.2	11.2
L-lysine	18.0	18.0
L-histidine	3.3	3.3
L-leucine	11.1	11.1
L-isoleucine	8.2	8.2
L-valine	8.2	8.2
L-threonine	8.2	8.2
L-tryptophan	1.8	1.8
DL-methionine	8.6	1.7
Glutamic acid	27.0	33.9
L-phenylalanine	11.6	11.6
Glycine	23.3	23.3
Dextrose	200.0	200.0
Dyetrose	50.0	50.0
Cornstarch	432.5	432.5
Cellulose fiber	50.0	50.0
Choline bitartrate	2.0	2.0
Vitamin mix #300050	10.0	10.0
Mineral mix #200000	35.0	35.0
Corn oil	80.0	80.0

[a]Energy content of control and methionine-restricted diets is 15.96 kJ/g.

substantial. In 2011, we reported the first proof of concept study to evaluate the safety and efficacy of dietary MR in humans with metabolic syndrome and found that restricting methionine for 16 weeks increased fat oxidation and reduced hepatic lipid content (Plaisance et al., 2011). This was accomplished using the medical food, Hominex-2, originally developed to provide nutritional support for patients with homocystinuria or hypermethioninemia. Although the significance was not recognized at the time of our study, Hominex-2 contains cysteine, and as we recently showed (Wanders et al., 2016), it is likely to have reversed key beneficial effects of dietary MR, including the induction of hepatic FGF21. A second, equally substantial impediment to implementing dietary MR in humans using Hominex-2 is that it is formulated using highly unpalatable, elemental amino acids that led to poor compliance and extensive withdrawal from the study (Plaisance et al., 2011). In the present work we provide a viable path to solving the palatability issue by subjecting intact casein to mild oxidative conditions to selectively delete methionine and cysteine. Using the oxidized casein to formulate methionine-restricted diets, we report here that an MR diet based on oxidized casein faithfully reproduced the physiological, biochemical, and transcriptional responses that are produced by an elemental amino-acid-based MR diet. Collectively, these findings demonstrate for the first time that dietary MR can be effectively implemented using casein after selective oxidative reduction of methionine.

RESULTS

Body weight, body composition, and energy balance

The amino acid and macronutrient composition of the elemental control (Ele Con) and Ele MR diets are provided in Table 1, whereas the formulation strategy and component composition (e.g., macronutrient and amino acids) of the Cas Con and Ox Cas MR diets are described in the STAR Methods and provided in Table 2, Figures 5A, 5B, S1A, and S1B. Although the source of the amino acids differed between the elemental amino-acid-based and casein-based diets, they were formulated to provide comparable amounts of total amino acids (e.g., ~14%) and comparable energy content (e.g., ~16 kJ/g; see Tables 1 and 2). To assess the ability of the Ox Cas MR diet to fully recapitulate the effects of the Ele MR diet on energy balance, body composition, biomarkers of metabolic health, and transcriptional effects in liver and white adipose tissue, comprehensive metabolic phenotyping was conducted on mice consuming

Table 2. Composition of the casein control (CAS CON) and oxidized casein MR (OX CAS MR) diets[a]

Ingredient	Concentrations in CAS CON diet (g/kg diet)	Concentrations in OX CAS MR diet (g/kg diet)
Control casein	141.00	0.00
Oxidized casein	0.00	153.00
DL-methionine[b]	3.58	0.23
L-lysine[c]	10.45	6.81
L-tryptophan[d]	1.68	0.17
Dextrose	200.00	200.00
Dyetrose	50.00	50.00
Cornstarch	419.90	405.90
Cellulose fiber	50.00	50.00
Choline bitartrate	2.00	2.00
Vitamin mix #300050	10.00	10.00
Mineral mix #200000	35.00	35.00
Corn oil	80.00	80.00

[a]From the Covance amino acid analysis, the protein content of the control casein was 88.8 g/100g and 80.1 g/100g for the oxidized casein. The difference is moisture content of the two proteins. To equalize the amount of protein added to each diet and match the amino acid content of the elemental diets, 141 g of Control Casein was added to each kg of the CON CAS diet and 153 g of oxidized casein was added to each kg of the OX CAS MR diet. The energy content of both diets is 16.0 kJ/g.

[b]DL-methionine (5.02 g) was added to the casein control diet to produce a final methionine concentration of 0.86% that matched the methionine concentration in the elemental control diet. DL-methionine (1.47 g) was added to the oxidized casein MR diet to produce a final methionine concentration of 0.17% that matched the methionine concentration of the elemental MR diet.

[c]L-lysine-HCl (7.57 g) was added to the casein control diet to produce a final lysine concentration of 1.8%. L-lysine HCL (11.19 g) was added to the oxidized casein MR diet to produce a final lysine concentration of 1.8%. This matched the lysine concentration in the elemental diets.

[d]L-tryptophan (1.515 g) was added to the oxidized casein MR diet to produce a final tryptophan concentration of 0.17% to match the tryptophan level in the casein control diet.

the two methionine-restricted experimental diets and the corresponding elemental and casein-based control diets. The initial body weight and body composition of all four dietary groups did not differ at the beginning of the study (Figures 1A–1C), and the two MR diets (e.g., Ele MR and Ox Cas MR) produced a comparable decrease in the accumulation of body weight, lean mass, and fat mass over the course of the 8-week study (Figures 1A–1C). In addition, the beginning body weights and composition did not differ among the four groups, whereas the final body weights and composition were comparable between the two control groups and between the two experimental groups (Figures 1A–1C). The cumulative food intake over time did not differ among any of the groups for the first 2 weeks, but by the third week, the Ele MR group had consumed significantly more food than the Ele Con group (Figure 1D). A similar pattern was observed between the two casein-based diets, with a higher cumulative intake detected in the Ox Cas MR group compared with the Cas Con group after 3 weeks and all weeks thereafter (Figure 1D). Cumulative intake did not differ between the Ele Con and Cas Con groups during the study or between the Ele MR and Ox Cas MR groups at any time point (Figure 1D). Water intake in the Ele MR and Ox Cas MR groups was significantly higher than their corresponding control groups after 2 weeks and at all subsequent time points (Figure 1E). The increased water intake observed in the Ele MR and Ox Cas MR groups was of a comparable magnitude and did not differ at any time point between these two groups (Figure 1E). In contrast, water intake in the two control groups averaged about 5 mL/day throughout the study and did not differ at any time point (Figure 1E). Average EE was measured at the end of the study continuously over three days, and average daytime and nighttime EE was compared by ANCOVA. The daytime EE did not differ between Ele Con and Cas Con groups, but the two MR diets produced a comparable 30%–40% increase in daytime EE relative to their respective control groups (Figure 1F). Figure 1F also shows that the daytime EE in the Ele MR and Ox Cas MR did not differ. At night when the mice are active and eating, nighttime EE in the two control groups was 10% higher than their corresponding daytime EEs (Figure 1F). The Ele MR diet

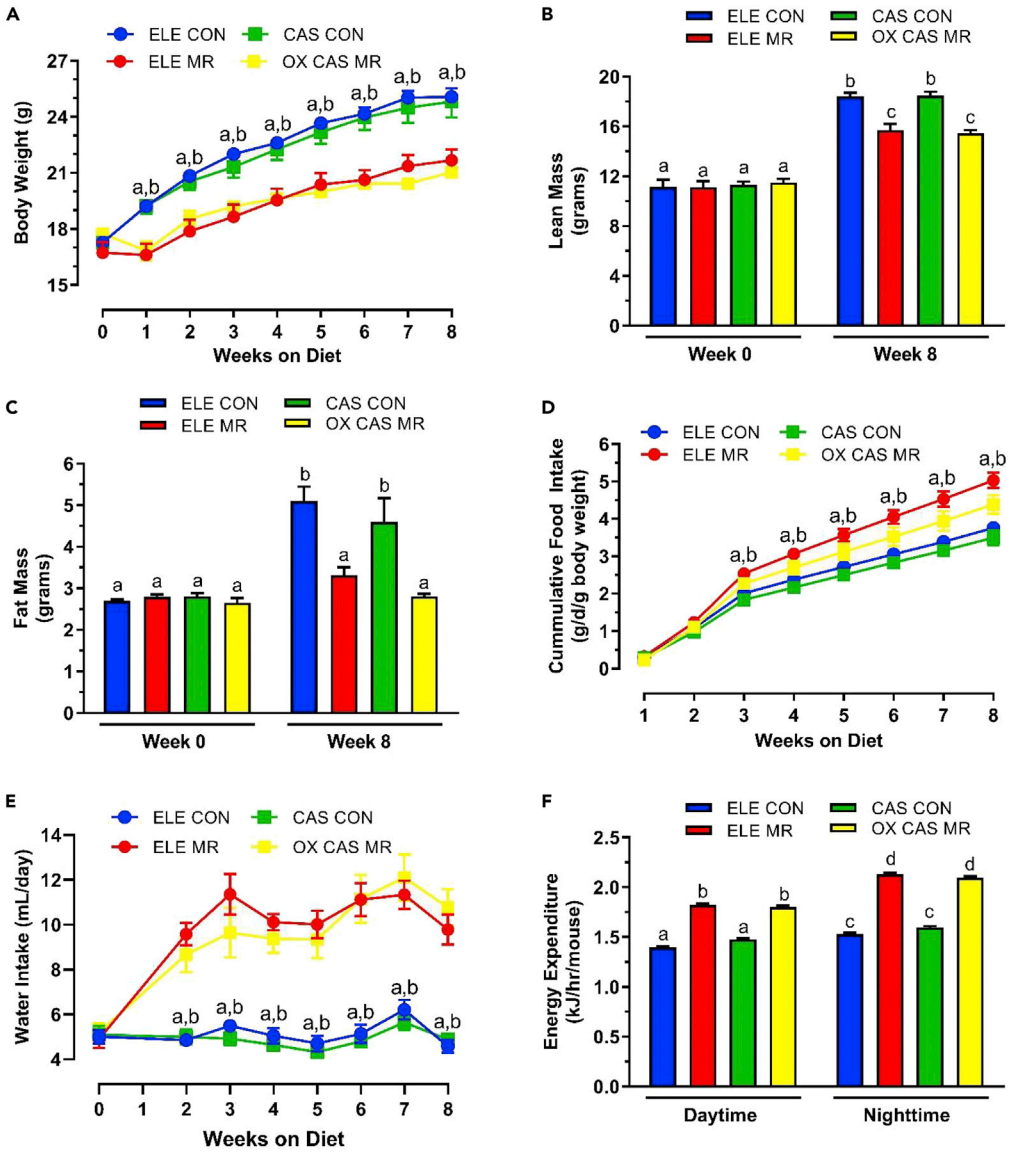

Figure 1. Dietary effects on energy balance

Acute and chronic effects of elemental dietary MR (Ele MR) and oxidized casein MR (Ox Cas MR) diets on body weight (A), lean body mass (B), fat mass (C), cumulative food intake (D), water intake (E), and energy expenditure (F). Body weight, food intake, and water intake were analyzed using a repeated measures one-way ANOVA, and means annotated with letters differ from their corresponding control group (A and D) or MR group (E) at $p < 0.05$. The mean values annotated with an "a" represent the comparison of the Ele MR to Ele Con means at each time point, and the means annotated with a "b" represent the comparison of the Ox Cas MR to Cas Con means. The annotation letters for both Ele MR and Ox Cas MR are placed above the Ele MR means for clarity. Endpoint analyses of body composition (B and C) were compared with a two-way ANOVA, and means with different letters differ between time point and/or dietary group. Mean daytime and nighttime EE in the four groups were compared using a two-way ANOVA, and means annotated with different letters differ between time of day and/or dietary group. Mean daytime and nighttime EE was calculated from the measurements made over a period of 3 days using ANCOVA as described in STAR Methods. All values are expressed as mean ± SEM for eight mice from each dietary group.

produced a 40% increase in nighttime EE compared with the Ele Con group, whereas the Ox Cas MR diet increased nighttime EE by 31% relative to Cas Con (Figure 1F). Collectively, the two MR diets produced comparable increases in daytime and nighttime EE compared with their respective control groups.

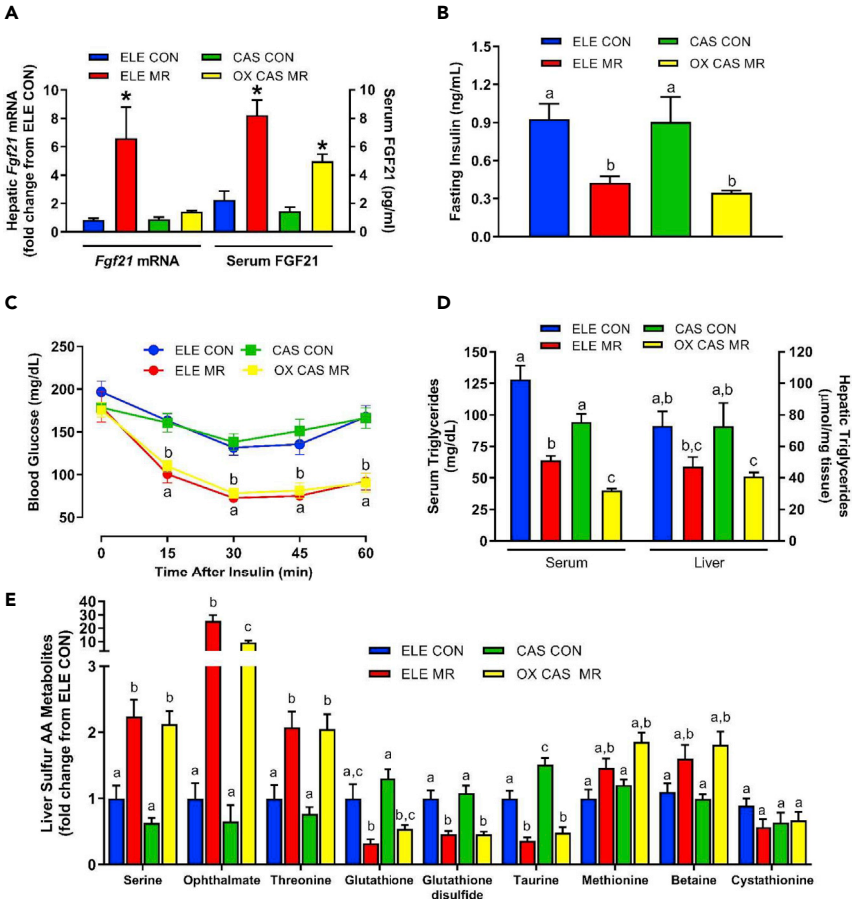

Figure 2. Dietary effects on endocrine biomarkers and hepatic metabolomics

Chronic effects of elemental dietary MR (Ele MR) and oxidized casein MR (Ox Cas MR) diets on circulating and hepatic FGF21 levels (A), fasting insulin (B), insulin-dependent glucose clearance (C), serum and hepatic triglycerides (D), and liver sulfur amino acid metabolites (E). The respective endpoints were analyzed with a one-way ANOVA, and means annotated with different letters differ at $p < 0.05$. The time points within the insulin tolerance test were compared within dietary groups at each time point using a repeated measures one-way ANOVA, and means annotated with different letters differ from their corresponding dietary control groups at that time point. All values are expressed as mean ± SEM for eight mice from each dietary group.

Endocrine and biochemical responses to the diets

The Ele MR diet produced a 7.8-fold increase in hepatic *Fgf21* mRNA compared with Ele Con and a 3.7-fold increase in serum FGF21 relative to the Ele Con group (Figure 2A). The Ox Cas MR diet also produced a significant 3.4-fold increase in serum FGF21 compared with the Cas Con group, but the increase in hepatic *Fgf21* mRNA produced by the Ox Cas MR diet was only 1.6-fold and not significant (Figure 2A). In contrast, both the Ele MR and Ox Cas MR diets produced a comparable decrease in fasting insulin compared with their respective control groups (Figure 2B). The ability of a fixed dose of insulin to lower blood glucose was also comparably enhanced by both the Ele MR and Ox Cas MR diets (Figure 2C). The Ele MR diet produced a significant decrease in serum triglyceride levels relative to Ele Con, but the decrease in hepatic triglyceride levels produced by the Ele MR diet was not significant (Figure 2D). In contrast, the Ox Cas MR diet produced a significant decrease in both serum triglycerides and hepatic triglyceride levels relative to the Cas Con group (Figure 2D). The two MR diet formulations are essentially devoid of cysteine and contain 5-fold less methionine than their respective control diets, so a key goal of the experiment was to assess diet-induced changes in key metabolites of methionine metabolism in the liver. Metabolites of the sulfur amino acid metabolism pathway previously shown to be affected by dietary MR (Ghosh et al., 2017) were compared, and hepatic levels of serine, ophthalmate, and threonine were comparably increased by the Ele MR and Ox Cas MR diets relative to their corresponding control groups (Figure 2E). In contrast,

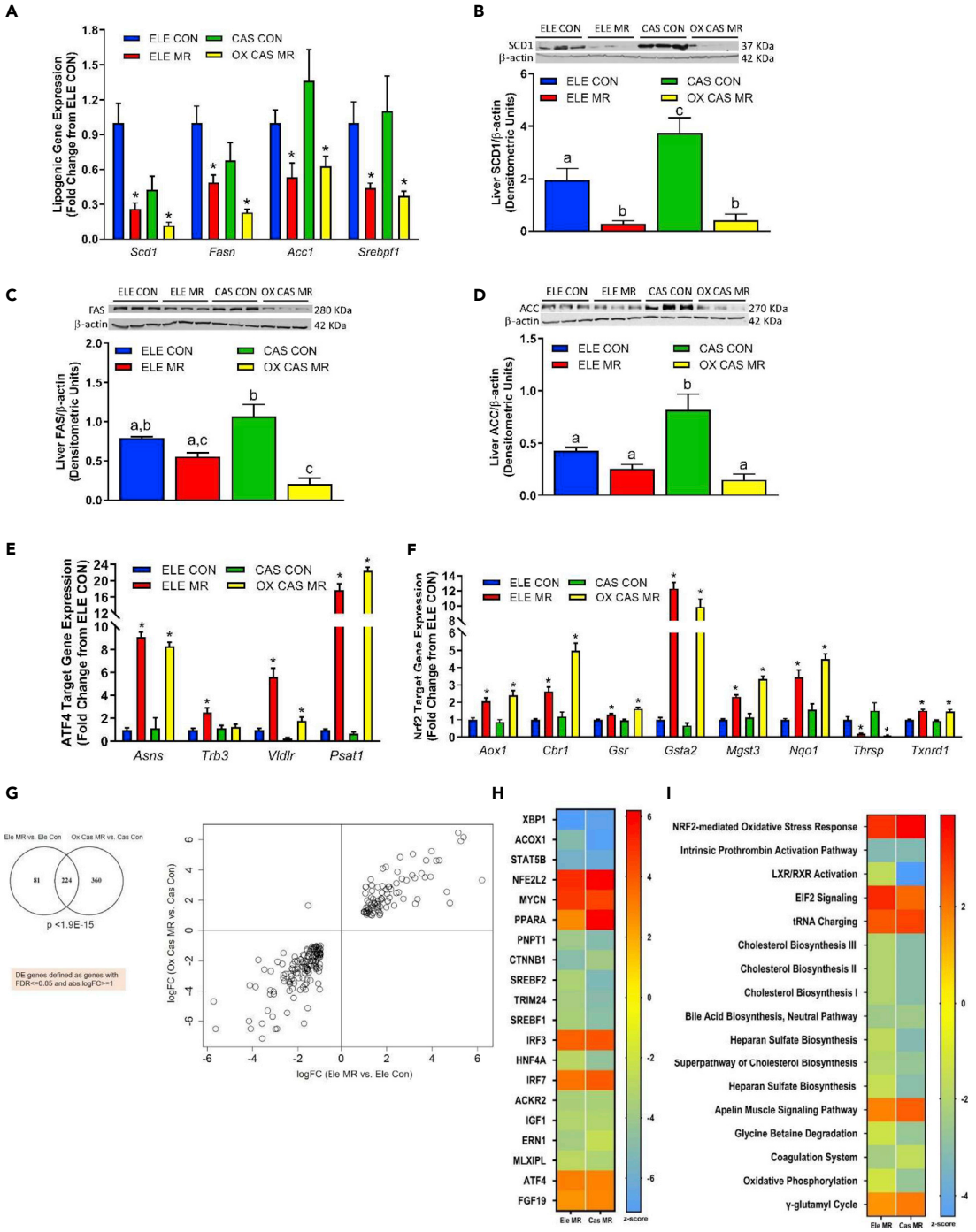

Figure 3. Contrast of dietary effects on hepatic gene expression

Transcriptional and translational responses to elemental dietary MR (Ele MR) and oxidized casein MR (Ox Cas MR) diets on liver lipogenic gene mRNA expression (A), lipogenic gene protein expression (B–D), activating transcription factor 4 (ATF4) target gene expression (E), nuclear factor erythroid 2-related factor 2 (NRF2) target gene expression (F), and overall differential gene expression (G–I). Hepatic gene expression was measured via qPCR, western blot, and RNAseq in livers harvested from mice after consuming elemental and casein-based diets for 8 weeks. Expression of hepatic lipogenic gene mRNAs (*stearoyl-CoA desaturase1 [Scd1], acetyl-CoA carboxylase [Acc], fatty acid synthetase [Fasn], and sterol regulatory element-binding transcription factor 1c [Srebpf1]*) were expressed relative to the Ele Con group and compared by one-way ANOVA (A). Means annotated with an asterisk differ from their corresponding control group. Hepatic SCD1 (B), FAS (C), and ACC (D) expression were measured by western blotting of 50 μg (SCD1) and 30 or 35 μg whole-cell extracts (ACC, FAS, respectively) using antibodies described in STAR Methods. β-actin served as a loading control and scanning densitometry was used to quantitate expression levels for each protein between groups. Means denoted with different letters differ at $p \leq 0.05$. The effect of the respective diets on

Figure 3. *Continued*

ATF4-sensitive genes (E) (*asparagine synthetase [Asns]*, *tribbles homolog 3 [Trb3]*, *very low-density lipoprotein receptor [Vldlr]*, *phosphoserine aminotransferase 1 [Psat1]*) and NRF2-sensitive genes (F) (*aldehyde oxidase 1 [Aox1]*, *carbonyl reductase 1 [Cbr1]*, *glutathione-disulfide reductase [Gsr]*, *glutathione S-transferase A2 [Gsta2]*, *microsomal glutathione S transferase 3 [Mgst3]*, *NAD(P)H quinone dehydrogenase 1 [Nqo1]*, *thioredoxin reductase 1 [Txnrd1]*) or decreases (e.g., *thyroid hormone responsive protein [Thrsp]*) in the liver. The mRNA level of each gene was expressed relative to the Ele Con group and compared by one-way ANOVA. Means annotated with an asterisk differ from their corresponding control group at $p \leq 0.05$. Comparison of differentially expressed genes in Ele MR and Ox Cas MR groups relative to their controls. Genes with adjusted p value ≤ 0.05 and absolute log2 fold-change ≥ 1 were considered as differentially expressed. The Venn diagram shows the overlap between the differentially expressed genes in Ele MR and Ox Cas MR groups (G). The observed overlap is highly significant ($p < 1.9 \times 10^{-15}$), and comparison of the direction of expression of the common differentially expressed genes shows that with the exception of 1 gene, all overlapping genes show similar direction of gene expression changes in the Ele MR and Ox Cas MR groups compared with controls (G). IPA upstream regulator analysis and canonical pathway analysis were conducted as described in STAR Methods. Heat maps showing the comparative effects of the two MR diets on the twenty most up- or downregulated transcription factors (H) and canonical pathways (I). Transcription factors and canonical pathways with an activation *Z* score ≥ 2 or ≤ 2 were considered to be significantly activated or inhibited at $p \leq 0.05$.

neither MR diet affected methionine, betaine, or cystathionine levels in the liver (Figure 2E). The two MR diets did produce the expected reductions of hepatic glutathione, glutathione disulfide, and taurine compared with the Ele Con and Cas Con groups, respectively (Figure 2E). Together, these findings show that the Ox Cas MR diet produced comparable metabolic and biochemical responses as the Ele MR diet.

Transcriptional effects of diets on lipogenic, activating transcription factor 4-sensitive and nuclear factor erythroid 2-related factor 2-sensitive genes in the liver

Dietary MR was previously shown to inhibit hepatic lipid synthesis (Hasek et al., 2013), so key genes associated with regulating these reactions were compared at the mRNA and protein levels. Based on real-time PCR measurements, the Ele MR diet produced the expected reductions in *stearoyl-CoA desaturase-1* (*Scd1*), *fatty acid synthetase* (*Fasn*), *acetyl-CoA carboxylase* (*Acc*), and *sterol regulatory element-binding transcription factor 1c* (*Srebpf1*) mRNA levels compared with the Ele Con group (Figure 3A) and a corresponding decrease in expression of hepatic SCD1 (Figure 3B) but not FAS (Figure 3C) or ACC (Figure 3D) protein levels compared with the Ele Con group. The Ox Cas MR diet was similarly effective in reducing *Scd1*, *Fasn*, *Acc*, and *Srebpf1* mRNA levels compared with the Cas Con group (Figure 3A), but it also produced significant reductions in the expression of hepatic SCD1 (Figure 3B), FAS (Figure 3C), and ACC (Figure 3D) protein levels compared with the Cas Con group. The findings make a compelling case that the Ox Cas MR diet fully recapitulates the effects of the Ele MR diet on hepatic lipid metabolism.

Previous work identified a group of hepatic genes associated with MR-induced effects on the ISR that are predicted to be mediated through activation of ATF4 and NRF2 (Wanders et al., 2016). Diet-induced changes in mRNA expression of four prototypical ATF4 target genes (*asparagine synthetase [Asns]*, *tribbles homolog 3 [Trb3]*, *very low-density lipoprotein receptor [Vldlr]*, *phosphoserine aminotransferase 1 [Psat1]*) were compared to assess the relative effects of the Ele MR and Ox Cas MR diets on ATF4 activation. As before, the Ele MR diet significantly increased the expression of all four genes relative to Ele Con (Figure 3E). The Ox Cas MR diet also increased expression of *Asns*, *Vldlr*, and *Psat* compared with the Cas Con group, but the increase in *Trb3* was not significant (Figure 3E). Assessment of NRF2-sensitive genes showed that the Ele MR and Ox Cas MR diets produced comparable increases (e.g., *aldehyde oxidase 1 [Aox1]*, *carbonyl reductase 1 [Cbr1]*, *glutathione-disulfide reductase [Gsr]*, *glutathione S-transferase A2 [Gsta2]*, *microsomal glutathione S transferase 3 [Mgst3]*, *NAD(P)H quinone dehydrogenase 1 [Nqo1]*, *thioredoxin reductase 1 [Txnrd1]*) or decreases (e.g., *thyroid hormone responsive protein [Thrsp]*) in expression of all eight genes relative to their corresponding Ele Con and Cas Con groups (Figure 3F). In addition, expression of all ATF4- and NRF2-sensitive genes was comparable between the Ele Con and Cas Con groups (Figures 3E and 3F).

Comparison of diet-induced differential gene expression in liver

To obtain a more in-depth and unbiased assessment of the respective effects of the two MR diets on hepatic gene expression, we used RNAseq in conjunction with bioinformatic analysis to interrogate the transcriptional responses in livers from mice on the respective diets. A comparison of gene expression in Ele MR versus Ele Con and Ox Cas MR versus Cas Con samples showed a statistically significant overlap of differentially expressed genes between the two MR treatments. A total of 305 and 584 genes were differentially expressed in the Ele MR and Ox Cas MR groups, respectively (absolute log fold-change ≥ 1 and

FDR ≤5%). Of these genes, 224 were differentially expressed in common among the two MR diets (Figure 3G), resulting in a highly significant overlap ($p < 1.9 \times 10^{-15}$, hypergeometric test). In addition, the expression of all but one of the overlapping genes was changed in the same direction in the two groups compared with controls (Figure 3G), suggesting similar mechanisms of gene regulation by the two MR treatments. Pathway enrichment analysis via Gene Set Enrichment Analysis (GSEA) also identified several pathways as enriched for differentially expressed genes in each of the comparisons performed, with some pathways showing enrichment in more than one comparison (Figure S3). We compared the top significant (FDR ≤5%) pathways from the Ele MR versus Ele Con and Ox Cas MR versus Cas Con comparisons and observed a statistically significant overlap among the pathways identified in common between the two comparisons. A total of 19 and 22 pathways were significantly enriched in the Ele MR and Ox Cas MR comparisons, respectively, with 10 pathways enriched in common among the two treatments ($p < 1.22 \times 10^{-7}$, hypergeometric test). These included pathways related to lipid metabolism, glutathione metabolism, and oxidative phosphorylation and translation, among others. The enrichment plots for four of these overlapping pathways are shown in Figure S3 to demonstrate the similarities in pathway gene rankings between the Ele MR and Ox Cas MR comparisons. A summary of the pathways identified by GSEA as differentially regulated is shown as heat maps in Figure S4. The values within each cell refer to the GSEA-derived normalized enrichment score (NES), an index of the extent of pathway regulation. NES is positive or negative if a pathway is upregulated or downregulated, respectively, and the last column shows the number of times a pathway has been identified as significantly regulated across the comparisons. Collectively, this approach to comparing the hepatic transcriptional responses to Ele MR and Ox Cas MR diets indicates a highly significant degree of overlap between the two diets.

To further explore the systems biology of hepatic transcriptional responses, Ingenuity's Pathway Analysis was used to screen differentially expressed genes against Ingenuity Knowledge Base's annotated database to detect predicted activation or inhibition of canonical pathways and upstream regulators. This algorithm predicts changes in transcription factor activity based on observed patterns of change in expression of genes known to be up- or downregulated by specific transcription factors. Heat maps were constructed to illustrate the comparative effects of the two MR diets on the twenty most up- or downregulated transcription factors (Figure 3H) and canonical pathways (Figure 3I). Transcription factors and canonical pathways with an activation *Z* score >2 or < −2 were considered to be significantly activated or inhibited, respectively. The three most highly inhibited hepatic transcription factors by MR were X-Box binding protein 1 (XBP1), acyl-CoA oxidase 1 (ACOX1), and signal transducer and activator of transcription 5B (STAT5B), and all three pathways are comparably inhibited by Ele MR and Ox Cas MR relative to the respective controls (Figure 3H). The three most activated transcription factors were nuclear factor erythroid 2-related factor 2 (NFE2L2), N-myc proto-oncogene (MYCN), and peroxisome proliferator-activated receptor alpha (PPARA), and again all three were comparably activated by the Ele MR and Ox Cas MR diets (Figure 3H). The remaining transcription factors were either activated or inhibited to lesser degrees, but more importantly, the relative effect of each transcription factor was similar between the two MR diets (Figure 3H). When canonical biological pathways were evaluated in terms of activation or inhibition, an identical conclusion was reached in terms of the relative effects of the two MR diets (Figure 3I). For example, the NRF2-mediated oxidative stress response, eukaryotic initiation factor 2 (eIF2) signaling, and tRNA charging were comparably activated by the Ele MR diet and Ox Cas MR diet (Figure 3I). A slight difference was observed with inhibited canonical pathways where the effect of the Ox Cas MR diet tended to be stronger than the inhibitory effect of the Ele MR diet (Figure 3I). However, when considered collectively over a wide range of canonical pathways and effects on multiple transcription factors, the responses to the two MR diets were highly comparable (Figures 3H and 3I).

Comparison of thermogenic gene expression in brown and inguinal white adipose tissue and differential gene expression in IWAT

The prototypical responses of brown and white adipose tissue to dietary MR involve an FGF21-dependent increase in sympathetic outflow that results in increased thermogenic gene expression, remodeling of cell morphology, and increased heat production (Patil et al., 2015; Wanders et al., 2017). Increased expression of *uncoupling protein 1* (*Ucp1*) mRNA and protein are archetypal markers of this process and were used to compare the efficacy of the two MR diets to enhance thermogenic potential. Figure 4A shows that Ele MR and Ox Cas MR produced comparable 5-fold increases in IWAT *Ucp1* mRNA relative to their respective control groups. The two MR diets also produced comparable increases in *Ucp1* mRNA in BAT (Figure 4A). The Ele MR and Ox Cas MR diets produced a small but significant increase in UCP1 protein expression in

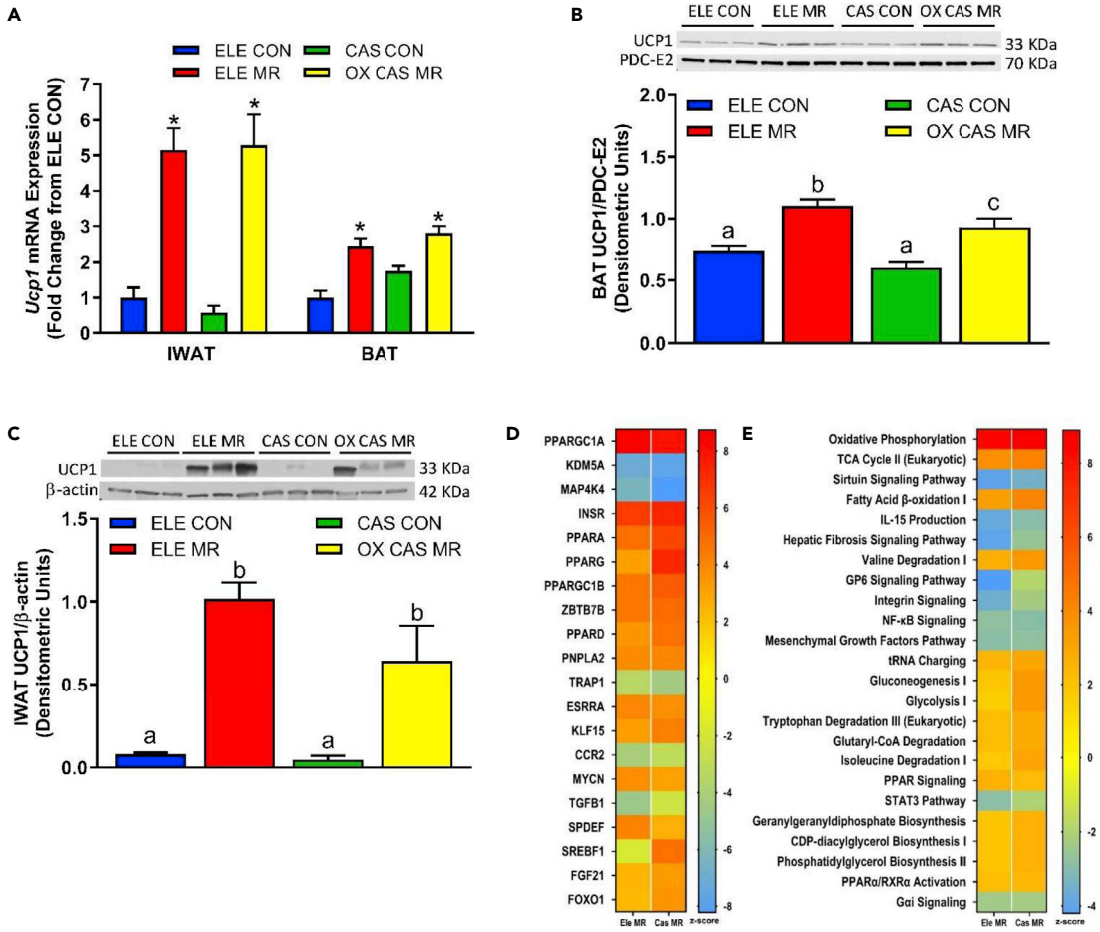

Figure 4. Contrast of dietary effects on inguinal white adipose tissue gene expression

Transcriptional and translational responses to elemental dietary MR (Ele MR) and oxidized casein MR (Ox Cas MR) diets on *uncoupling protein 1 (Ucp1)* mRNA expression in inguinal white (IWAT) and brown (BAT) adipose tissue (A), UCP1 protein expression in BAT (B) and inguinal WAT (C), and overall differential gene expression in inguinal WAT (D and E). IWAT and BAT *Ucp1* mRNA expression were measured by qPCR and western blot, and differential gene expression in IWAT was measured using RNAseq as described in STAR Methods. Expression of *Ucp1* mRNA was expressed relative to the Ele Con group and compared by one-way ANOVA. Means annotated with an asterisk differ from their corresponding control group at $p < 0.05$ (A). UCP1 protein expression was measured in the two tissues by western blotting using an antibody described in STAR Methods. PDC-E2 served as a loading control for BAT (B), whereas β-actin served as a loading control for IWAT (C). Scanning densitometry was used to quantitate expression levels for UCP1 protein between tissues and dietary groups, and means denoted with different letters differ at $p \leq 0.05$ (B and C). IPA upstream regulator analysis and canonical pathway analysis were conducted with differentially expressed genes in Ele MR and Ox Cas MR groups relative to their controls, as described in STAR Methods. Heat maps showing the comparative effects of the two MR diets on the twenty most up- or downregulated transcription factors (D) and canonical pathways (E). Transcription factors and canonical pathways with an activation *Z* score ≥ 2 or ≤ 2 were considered to be significantly activated or inhibited at $p \leq 0.05$.

BAT (Figure 4B) and a larger increase in UCP1 expression in IWAT (Figure 4C). Together these findings show that the two MR diets produced comparable increases in UCP1 expression relative to their respective control groups.

A comprehensive comparison of the transcriptional responses of IWAT to the MR diets by RNAseq and bioinformatic analysis showed a significant overlap of differentially expressed genes between the two MR diets. Pathway enrichment via GSEA identified several pathways as enriched for differentially expressed genes in each of the comparisons performed, with some pathways showing enrichment in more than one comparison (Figure S5). We compared the top significant (FDR $\leq$5%) pathways from the Ele MR versus Ele Con and Ox Cas MR versus Cas Con comparisons and observed a statistically significant overlap among the pathways identified in common between the two comparisons. A total of 59 and 84 pathways were significantly enriched in the Ele MR and Ox Cas MR comparisons, respectively, with 45 pathways enriched in

common among the two treatments (overlap $p < 9.58 \times 10^{-11}$) (Figure S5). These included pathways related to oxidative phosphorylation, citrate cycle metabolism, and fatty acid metabolism. The enrichment plots for these three overlapping pathways are shown in Figure S5 and demonstrate the similarities in pathway gene rankings between the Ele MR and Ox Cas MR comparisons. A summary of the pathways identified by GSEA as differentially regulated is shown as heat maps in Figure S6. Collectively, this approach to comparing the transcriptional responses in IWAT between Ele MR and Ox Cas MR diets indicates a highly significant degree of overlap between the two diets.

The Ingenuity Pathway Analysis was again used to screen differentially expressed genes against Ingenuity Knowledge Base to predict activation or inhibition of canonical pathways and upstream regulators. Heat maps showing the comparative effects of the two MR diets on the twenty most up- or downregulated transcription factors (Figure 4D) and canonical pathways (Figure 4E) show that the primary effects on both categories involved activation. Eleven upstream regulators were activated with z-scores in excess of 4, whereas only 5 of the 20 upstream regulators were inhibited (Figure 4D). Oxidative phosphorylation was the most highly activated canonical pathway, and both MR diets comparably activated this pathway (Figure 4E). TCA cycle metabolism, fatty acid oxidation, PPAR signaling, and several pathways involving amino acid metabolism were also activated by both MR diets in IWAT (Figure 4E). Nine of the twenty canonical pathways were inhibited, and in almost all cases, the Ele MR and Ox Cas MR diets produced similar degrees of inhibition of those pathways (Figure 4E). When the transcription factors and canonical pathways that were most significantly affected by the two MR diets were compared, the Ele MR and Ox Cas MR diets produced highly comparable responses in IWAT. The transcriptional effects of the two MR diets span a range of biological responses, and the overall conclusion at the molecular level in both liver and IWAT is that the two MR diets produced highly comparable transcriptional effects. Therefore, the collective result of our phenotyping of the full range of dietary responses is that the Ox Cas MR diet faithfully reproduces the biological effects of the Ele MR diet.

DISCUSSION

Implementation of dietary MR in a pre-clinical context requires a 5-fold reduction of dietary methionine and the elimination of cysteine. Essentially all studies on MR to date use diets formulated from elemental amino acids that reduce the final methionine concentration to 0.17%. Rats and mice readily adapt to these amino-acid-based diets, and the health benefits of MR on longevity (Orentreich et al., 1993; Richie et al., 1994), heath span (Malloy et al., 2006), and biomarkers of metabolic health have been rigorously documented over the last 20 years (Ables et al., 2012; Forney et al., 2020; Ghosh et al., 2017; Hasek et al., 2010, 2013; Patil et al., 2015; Perrone et al., 2009, 2012b; Plaisance et al., 2010; Stone et al., 2021). The effects include a reproducible series of transcriptional, biochemical, physiological, and behavioral responses that culminate in reduced fat deposition, enhanced insulin sensitivity, reduced circulating lipids, and prevention or reversal of obesity. Many of these studies also employed mechanistic approaches to assess the role of various sensing/signaling molecules, enzymes, and transcription factors in mediating the biological effects of dietary MR. A critical advance in our understanding of the underlying biology came with the recognition that hepatic sensing of reduced methionine led to transcriptional activation and release of FGF21 from the liver (Stone et al., 2014). The resulting increase in serum FGF21 is essential to many of MR's beneficial metabolic effects, and these effects accrue from a combination of indirect effects of FGF21 signaling in the brain and direct effects of FGF21 in adipose tissue (Forney et al., 2020; Wanders et al., 2017). MR also reduces the capacity of the liver to synthesize and export lipid through direct transcriptional mechanisms (Hasek et al., 2013). Collectively, this body of work makes a compelling case that dietary MR produces a reproducible and highly beneficial metabolic phenotype in studies with rats and mice. Most importantly, these beneficial responses do not require limitation of food intake, as the MR diet produces its full range of metabolic effects when provided *ad libitum*. In the present work, a novel approach to implementing dietary MR is tested that circumvents the difficulties of using elemental amino-acid-based diets.

Dietary strategies that produce weight loss without food restriction represent an appealing approach to treat metabolic disease. Although lifestyle modifications that require chronic reductions in energy intake are effective in producing short-term weight loss and metabolic improvements, they also suffer from high rates of recidivism and weight regain due to noncompliance. Given that the beneficial effects of dietary MR do not require food restriction, in 2011 we tested the efficacy and safety of dietary MR as a treatment for metabolic disease using the medical food, Hominex-2 (Plaisance et al., 2011). Hominex-2 was developed by Abbott Labs (Abbott Park, IL, USA) for patients with hypermethionemia and is formulated

using elemental amino acids minus methionine. However, we found that the presence of cysteine in Hominex-2 spared methionine and limited the severity of the methionine restriction (Plaisance et al., 2011). This coincides with the findings from earlier pre-clinical studies showing that the presence of cysteine compromised the biological efficacy of dietary MR (Elshorbagy et al., 2011; Wanders et al., 2016). However, we concluded that even if cysteine was eliminated from Hominex-2, the more significant impediment to its use in implementing dietary MR would be the low palatability, poor compliance, and high withdrawal rates caused by the bad taste of elemental amino acids (Plaisance et al., 2011). The potential solution to the palatability problem being tested in the present work involves selectively targeting methionine in intact proteins using mild oxidation. The goal was to maintain the palatability of an intact protein while simultaneously reducing the available methionine and cysteine to therapeutic levels.

It has been known for 70 years that methionine is readily degraded to methionine sulfoxide by hydrogen peroxide (Matsuo, 1953), and subsequent work showed that methionine and cysteine residues in intact proteins were also subject to oxidation by hydrogen peroxide (Slump and Schreuder, 1973). The authors determined the extent of methionine and cysteine oxidation chemically, followed by biological assay of the nutritive value of the oxidized proteins (Slump and Schreuder, 1973). They concluded that the methionine in casein and fish meal was oxidized almost completely under their conditions. Similarly, Anderson et al. (Anderson et al., 1975) evaluated the ability of rapeseed flour to support the growth of weanling rats after oxidation with hydrogen peroxide. They found that without methionine supplementation (e.g., 0.15%–0.30%), the oxidized protein would not support growth. Other studies showed that tryptophan and lysine were also reduced in casein by hydrogen peroxide (Nielsen et al., 1985), so our goal was to identify the minimal oxidative conditions sufficient to remove methionine and cysteine from casein while causing little additional damage to the protein. Through an iterative process using a range of reaction conditions (e.g., pH, H_2O_2 concentration, temperature), we identified conditions that were sufficient to reduce methionine and cysteine to near zero while producing a minimum of effects on all other amino acids. Like methionine, tryptophan is very susceptible to oxidation, so it too was totally degraded in the oxidized protein. The only other amino acid that was significantly affected was lysine, and it was reduced by 35% compared with untreated casein (Figure 5).

Based on amino acid analysis of the control and oxidized casein (Figures S1 and S2), the oxidized casein was used to formulate the Ox Cas MR diet by adding back lysine and tryptophan to their original levels in control casein and adding sufficient methionine to bring the final concentration in the diet to 0.17%. Our experimental strategy was also to balance macronutrient levels among our four diets so that total amino acids, carbohydrate, and fat provided in the Ox Cas MR and Cas Con diets were closely matched to the amounts in our Ele Con and Ele MR diets. The success of this strategy is borne out by a comparison of essentially every endpoint being compared between the Ele Con and Cas Con groups. With rare exception the two control groups were similar in almost every endpoint measured during the study. The value of this similarity comes in evaluating the ability of the Ox Cas MR diet to reproduce the biological responses of the Ele MR diet, and in both cases the efficacy of the two experimental diets is assessed relative to their respective control groups. And within the margin of error, the Ox Cas MR diet produced a decrease in body weight, a decrease in lean mass, a decrease in fat mass, an increase in food intake, an increase in water intake, an increase in EE, an increase in serum FGF21, a decrease in fasting insulin, an improvement in insulin-dependent glucose clearance, and a decrease in serum triglycerides relative to the Cas Con group that did not differ from the corresponding effects of the Ele MR diet on these variables relative to the Ele Con group. The two diets also produced comparable changes in intermediates of sulfur amino acid metabolism in the liver. The similar efficacy of the Ox Cas MR diet and Ele MR diets also included their effects on thermogenic genes and proteins in adipose tissue, lipogenic genes and proteins in the liver, ATF4-sensitive genes in the liver, and NRF2-sensitive genes in the liver. A more rigorous and unbiased evaluation of the respective transcriptional effects of the two MR diets (e.g., RNAseq) provided comprehensive evidence that the top 20 most highly affected transcription factors and canonical pathways were similarly affected by the Ox Cas MR diet and Ele MR diets relative to their respective control groups in both liver and IWAT. In addition, examination of these transcriptional responses provide links to how the two MR diets affected the metabolic phenotype of mice in each group. For example, the transcription factor XBP1 was highly and similarly inhibited in livers from the Ox Cas MR group and Ele MR group (Figure 3H). Although XBP1 is an important regulator of the unfolded protein response, it also plays a key role in regulating hepatic lipogenic gene expression (Lee et al., 2008). Although the pathway through which the MR diets act to inhibit XBP1 activity is not yet known, its inhibition could be a key mechanism linking the MR diet to its potent inhibition of

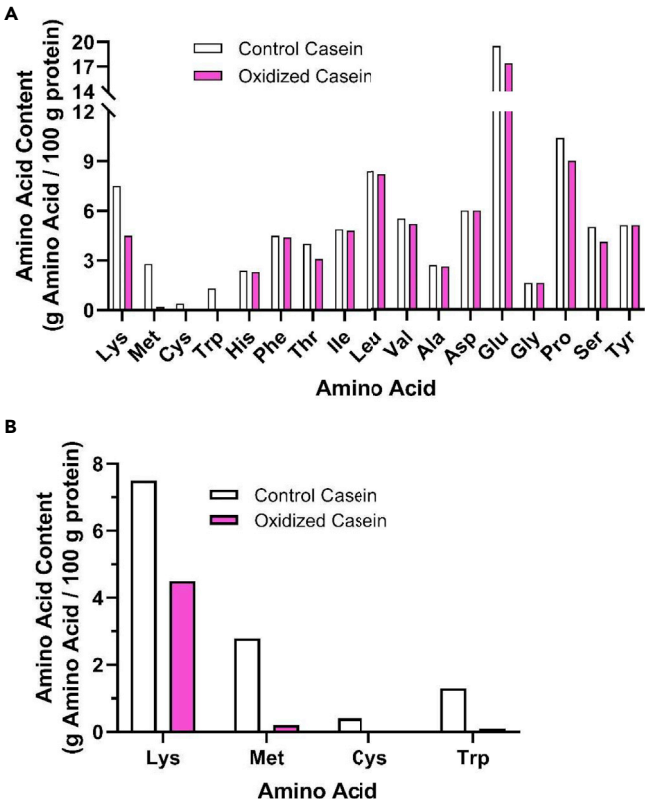

Figure 5. Amino acid analysis of the control casein and oxidized casein used to construct the control casein diet and the oxidized casein MR diet

Oxidation of casein was conducted as described in the STAR Methods, and Covance Inc. conducted the amino acid analysis (see Figures S1 and S2). Comparison of all amino acids in the profile presented in 5A and exploded view of the four amino acids significantly impacted by the oxidation procedure presented in 5B.

hepatic lipogenesis (Hasek et al., 2013). The transcription factor NRF2 (encoded by Nfe2l2) induces the expression of numerous antioxidant genes in the liver (Wanders et al., 2016), and the reduction of glutathione produced by both MR diets could explain the potent activation of hepatic NRF2 by both diets (Figures 3H and 3I). However, as reported by Rooney et al. (Rooney et al., 2018), the potent inhibition of hepatic STAT5B by both MR diets may provide another functional link to NRF2 activation in each case (Figure 3H). In addition, Vluggens and coworkers (Vluggens et al., 2010) demonstrated crosstalk between ACOX1 and PPARα through regulated peroxisome proliferation, with reduced ACOX1 function causing increased peroxisome proliferation. Therefore, the observed inhibition of ACOX1 by both MR diets could be functionally linked to the enhanced PPARα activation common to both MR diets through increased formation of peroxisome proliferators (Figure 3H). Lastly, the highly activated eIF2 signaling and tRNA charging produced by both MR diets is fully consistent with the activation of the ISR by dietary MR (Stone et al., 2021). Future studies will be required to better understand the sensing and signaling systems linking restriction of dietary methionine to these highly integrated transcriptional responses, but for purposes of the work undertaken here, it seems clear that dietary MR produced with the Ox Cas MR diet faithfully recapitulates the transcriptional responses of the Ele MR diet.

It should also be noted that there were several significant differences between the lipid metabolism phenotype of mice on the elemental diets and mice on the casein-based diets. For example, protein expression of the lipogenic enzymes, SCD1 and ACC, was significantly higher in liver from the Con Cas group compared with the Ele Con group (Figures 3B and 3D). These differences did not translate into higher serum or hepatic triglyceride levels between the respective control groups, although the Ox Cas MR diet did produce a more significant lowering of serum triglyceride than the Ele MR diet (Figure 2D). Another notable difference in markers of hepatic lipid metabolism was the more significant inhibition of SREBF2 and LXR/RXR

activation by the Ox Cas MR diet (Figures 3H and 3I). Given that LXR functions as a sensor of cellular cholesterol concentration and induces the transcription of key cholesterol shuffling vehicles (e.g., ABCA1 and ApoE), although SREBP2 has long been viewed as primarily responsible for activation of genes involved in cholesterol synthesis, it is interesting that the Ox Cas MR diet produces a more notable inhibition of both SREBF2 and LXR/RXR, and this is reflected by more effective inhibition of cholesterol biosynthesis by the Ox Cas MR diet than the Ele MR diet (Figure 3I). Although it is beyond the scope of the current work to explore this observation, it does emphasize that the responses to the different diets are not uniform. Previous work has reported that dietary MR produces a lowering of cholesterol in serum and liver (Perrone et al., 2009, 2012b), so an interesting line of inquiry will be to examine the relative effects of these diets on cholesterol shuffling versus synthesis in the liver.

Collectively, our studies provide compelling new evidence for the feasibility of developing therapeutic diets that restrict dietary methionine to biologically beneficial levels without the need to formulate such diets using mixtures of individual, highly unpalatable amino acids. Our findings demonstrate that under well-defined conditions, mild oxidation of intact proteins selectively degrades methionine and cysteine to near completion, allowing the subsequent use of the oxidized protein to construct more palatable diets with defined concentrations of methionine. Although tryptophan, and to a minor degree lysine, is also degraded under these conditions, the amino acids are easily restored to their original levels during diet formulation. The most significant finding from the present work is that experimental manipulation of methionine concentration in casein into the range previously shown to be effective was able to faithfully reproduce all the biological responses produced by elemental methionine manipulation. There were essentially no off-target responses among all the variables monitored, leading to the conclusion that the degradation products of sulfur amino acid oxidation (e.g., methionine sulfoxide, cysteic acid) were of no nutritive value and excreted through normal channels. The path to translation of the current findings to therapeutic diets will require studies to establish that mild oxidation has a minimal effect on the palatability of the proteins that will be used to construct a methionine-restricted diet. The complexity of the human diet, with multiple sources of animal and plant proteins contributing varying amounts of methionine and cysteine, promises to make implementation of the approach described here challenging. However, the far-reaching negative impact of metabolic disease in our society argues for vigorous pursuit of the basic concept that limiting methionine intake to a specific range could be highly beneficial to human health. A more practical solution in the short term might be to develop a limited but highly palatable group of modified proteins that could be the basis of a therapeutic diet that is consumed under medical supervision for a specified interval. It will be essential to enlist the expertise of food scientists to overcome the technical challenges of creating a diverse set of palatable foodstuffs, working in conjunction with nutritionists to develop the methionine accounting software needed to keep methionine intake within the desired range.

Limitations of the study

The path to translational implementation of dietary MR using the approach described here will require producing and testing the acceptability and efficacy of the diverse set of proteins that make up the human diet. Although proof of concept testing was successful here with casein, oxidative conditions that produce degradation of methionine with minimal effects on other amino acids will have to be established for other proteins. In the current work, casein was solubilized in heated water at low pH to achieve full oxidation of methionine with dilute H_2O_2, but many protein sources in the human diet are animal muscle that are consumed in solid form after cooking (e.g., steak, fish, poultry). It will be challenging to achieve full oxidation for amino acids not on the surface of the meat, so alternative oxidizing agents (e.g., ozone) and methods will need to be developed. And in every case, the palatability will need to be established and preserved. Another significant limitation of the current work involves the differing amino acid composition of different proteins. A major unanswered question is whether methionine restriction after oxidation of other protein sources will be as effective as methionine restriction using casein. This question will have to be systematically answered for each new protein source to establish that producing dietary MR with a diet consisting of multiple protein sources is as effective as what we observed here with a single protein source.

In addition, metabolic disease is a growing problem in companion animals, so the potential benefits of a therapeutic MR diet for dogs and cats is appealing. Although the range of proteins used to constitute pet food diets is less broad, it will still be necessary to conduct proof of concept studies that establish the palatability and metabolic efficacy of companion animal diets produced using the experimental approach described here. Species-specific nutrition expertise will be required to supplement the formulated diets

accordingly after careful evaluation of the impact of oxidation on these protein sources. Taurine supplementation in the diet of cats is a representative example where oxidation of animal proteins could produce other changes that could present problems if not considered.

STAR★METHODS

Detailed methods are provided in the online version of this paper and include the following:

- KEY RESOURCES TABLE
- RESOURCE AVAILABILITY
  - Lead contact
  - Materials availability
  - Data and code availability
- EXPERIMENTAL MODEL AND SUBJECT DETAILS
  - Formulation of elemental control and MR diets
  - Production of control and oxidized casein for diet formulation
  - Formulation of oxidized Casein MR and Casein control diets
  - Experimental animal protocol and metabolic phenotyping
- METHOD DETAILS
  - Indirect calorimetry
  - Insulin tolerance testing and tissue harvest
  - Triglyceride assay and serum hormones
  - Western blotting
  - RNA isolation and RNAseq
  - Preranked GSEA analysis
  - Ingenuity pathway analysis (IPA)
  - qPCR analysis
  - Metabolomics analysis
- QUANTITATIVE AND STATISTICAL ANALYSIS

SUPPLEMENTAL INFORMATION

Supplemental information can be found online at https://doi.org/10.1016/j.isci.2021.102470.

ACKNOWLEDGMENTS

We are grateful to Manda Orgeron for technical contributions to the conduct of this study. This work was supported BY NIH DK-096311 (TWG). This work also made use of the Genomics Core Facility supported by NIH P20-GM103528 (TWG), NIH P20 GM-135002 and NIH 2P30 DK072476. This research project used the Transgenic and Animal Phenotyping core facilities that are supported in part by the NORC (NIH 2P30 DK072476) and COBRE (NIH P20 GM-135002) center grants and by an equipment grant (S10OD023703) from the NIH. SG was supported in part by NIH 2 U54 GM104940 and from the Ministry of Health, National Medical Research Sciences, Singapore.

AUTHOR CONTRIBUTIONS

HF, KPS, LAF, SG, and TWG contributed to the writing and editing of the manuscript. HF, KPS, LAF, and LCS conducted experiments and associated mRNA and metabolite measurements. GCG produced the oxidized casein used to formulate the diets; and HF, KPS, SG, and TWG analyzed the data and produced the illustrations.

DECLARATION OF INTERESTS

Finley, J.W., Gettys, T.W., and Greenway, F.L. 2021—Palatable Foods for a Methionine-Restricted Diet. US Patent Application 61/831,189 filed June 5, 2013 and issued as US Patent 10,897,921 on January 26, 2021.

Received: February 25, 2021
Revised: March 29, 2021
Accepted: April 22, 2021
Published: May 21, 2021

REFERENCES

Ables, G.P., Perrone, C.E., Orentreich, D., and Orentreich, N. (2012). Methionine-restricted C57BL/6J mice are resistant to diet-induced obesity and insulin resistance but have low bone density. PLoS One *7*, e51357.

Anderson, G.H., Li, G.S., Jones, J.D., and Bender, F. (1975). Effect of hydrogen peroxide treatment on the nutritional quality of rapeseed flour fed to weanling rats. J. Nutr. *105*, 317–325.

Elshorbagy, A.K., Valdivia-Garcia, M., Mattocks, D.A., Plummer, J.D., Smith, A.D., Drevon, C.A., Refsum, H., and Perrone, C.E. (2011). Cysteine supplementation reverses methionine restriction effects on rat adiposity: significance of stearoyl-coenzyme A desaturase. J. Lipid Res. *52*, 104–112.

Finley, J.W., Gettys, T.W., and Greenway, F.L. (2021). Palatable foods for a methionine-restricted diet, U.S.P. Office (Board of Supervisors LSU).

Forney, L.A., Fang, H., Sims, L.C., Stone, K.P., Vincik, L.Y., Vick, A.M., Gibson, A.N., Burk, D.H., and Gettys, T.W. (2020). Dietary methionine restriction signals to the brain through fibroblast growth factor 21 to regulate energy balance and remodeling of adipose tissue. Obesity (Silver Spring) *28*, 1912–1921.

Ghosh, S., Forney, L.A., Wanders, D., Stone, K.P., and Gettys, T.W. (2017). An integrative analysis of tissue-specific transcriptomic and metabolomic responses to short-term dietary methionine restriction in mice. PLoS One *12*, e0177513.

Ghosh, S., Wanders, D., Stone, K.P., Van, N.T., Cortez, C.C., and Gettys, T.W. (2014). A systems biology analysis of the unique and overlapping transcriptional responses to caloric restriction and dietary methionine restriction in rats. FASEB J. *28*, 2577–2590.

Hasek, B.E., Boudreau, A., Shin, J., Feng, D., Hulver, M., Van, N.T., Laque, A., Stewart, L.K., Stone, K.P., Wanders, D., et al. (2013). Remodeling the integration of lipid metabolism between liver and adipose tissue by dietary methionine restriction in rats. Diabetes *62*, 3362–3372.

Hasek, B.E., Stewart, L.K., Henagan, T.M., Boudreau, A., Lenard, N.R., Black, C., Shin, J., Huypens, P., Malloy, V.L., Plaisance, E.P., et al. (2010). Dietary methionine restriction enhances metabolic flexibility and increases uncoupled respiration in both fed and fasted states. Am. J. Physiol. Regul. Integr. Comp. Physiol. *299*, R728–R739.

Jonsson, W.O., Margolies, N.S., Mirek, E.T., Zhang, Q., Linden, M., Hill, C., Link, C., Bithi, N., Zalma, B., Levy, J., et al. (2021). Physiological responses to dietary sulfur amino acid restriction are influenced by Atf4 status and biological sex. J. Nutr. https://doi.org/10.1093/jn/nxaa396.

Lee, A.H., Scapa, E.F., Cohen, D.E., and Glimcher, L.H. (2008). Regulation of hepatic lipogenesis by the transcription factor XBP1. Science *320*, 1492–1496.

Lee, B.C., Kaya, A., Ma, S., Kim, G., Gerashchenko, M.V., Yim, S.H., Hu, Z., Harshman, L.G., and Gladyshev, V.N. (2014). Methionine restriction extends lifespan of Drosophila melanogaster under conditions of low amino-acid status. Nat. Commun. *5*, 3592.

Lees, E.K., Krol, E., Grant, L., Shearer, K., Wyse, C., Moncur, E., Bykowska, A.S., Mody, N., Gettys, T.W., and Delibegovic, M. (2014). Methionine restriction restores a younger metabolic phenotype in adult mice with alterations in fibroblast growth factor 21. Aging Cell *13*, 817–827.

Liberzon, A., Birger, C., Thorvaldsdottir, H., Ghandi, M., Mesirov, J.P., and Tamayo, P. (2015). The Molecular Signatures Database (MSigDB) hallmark gene set collection. Cell Syst. *1*, 417–425.

Love, M.I., Huber, W., and Anders, S. (2014). Moderated estimation of fold change and dispersion for RNA-seq data with DESeq2. Genome Biol. *15*, 550.

Malloy, V.L., Krajcik, R.A., Bailey, S.J., Hristopoulos, G., Plummer, J.D., and Orentreich, N. (2006). Methionine restriction decreases visceral fat mass and preserves insulin action in aging male Fischer 344 rats independent of energy restriction. Aging Cell *5*, 305–314.

Malloy, V.L., Perrone, C.E., Mattocks, D.A., Ables, G.P., Caliendo, N.S., Orentreich, D.S., and Orentreich, N. (2013). Methionine restriction prevents the progression of hepatic steatosis in leptin-deficient obese mice. Metabolism *62*, 1651–1661.

Matsuo, Y. (1953). Degradation of methionine by hydrogen peroxide. Nature *171*, 1021–1022.

Miller, R.A., Buehner, G., Chang, Y., Harper, J.M., Sigler, R., and Smith-Wheelock, M. (2005). Methionine-deficient diet extends mouse lifespan, slows immune and lens aging, alters glucose, T4, IGF-I and insulin levels, and increases hepatocyte MIF levels and stress resistance. Aging Cell *4*, 119–125.

Nielsen, H.K., De Weck, D., Finot, P.A., Liardon, R., and Hurrell, R.F. (1985). Stability of tryptophan during food processing and storage. 1. Comparative losses of tryptophan, lysine and methionine in different model systems. Br. J. Nutr. *53*, 281–292.

Ogata, H., Goto, S., Sato, K., Fujibuchi, W., Bono, H., and Kanehisa, M. (1999). KEGG: Kyoto Encyclopedia of genes and Genomes. Nucleic Acids Res. *27*, 29–34.

Orentreich, N., Matias, J.R., DeFelice, A., and Zimmerman, J.A. (1993). Low methionine ingestion by rats extends life span. J. Nutr. *123*, 269–274.

Patil, Y.N., Dille, K.N., Burk, D.H., Cortez, C.C., and Gettys, T.W. (2015). Cellular and molecular remodeling of inguinal adipose tissue mitochondria by dietary methionine restriction. J. Nutr. Biochem. *26*, 1235–1247.

Perrone, C.E., Malloy, V.L., Orentreich, D.S., and Orentreich, N. (2012a). Metabolic adaptations to methionine restriction that benefit health and lifespan in Rodents. Exp. Gerontol. *48*, 654–660.

Perrone, C.E., Mattocks, D.A., Hristopoulos, G., Plummer, J.D., Krajcik, R.A., and Orentreich, N. (2008). Methionine restriction effects on 11β-HSD1 activity and lipogenic/lipolytic balance in F344 rat adipose tissue. J. Lipid Res. *49*, 12–23.

Perrone, C.E., Mattocks, D.A., Jarvis-Morar, M., Plummer, J.D., and Orentreich, N. (2009). Methionine restriction effects on mitochondrial biogenesis and aerobic capacity in white adipose tissue, liver, and skeletal muscle of F344 rats. Metabolism *59*, 1000–1011.

Perrone, C.E., Mattocks, D.A., Plummer, J.D., Chittur, S.V., Mohney, R., Vignola, K., Orentreich, D.S., and Orentreich, N. (2012b). Genomic and metabolic responses to methionine-restricted and methionine-restricted, cysteine-supplemented diets in Fischer 344 rat inguinal adipose tissue, liver and quadriceps muscle. J. Nutrigenet. Nutrigenomics *5*, 132–157.

Plaisance, E.P., Greenway, F.L., Boudreau, A., Hill, K.L., Johnson, W.D., Krajcik, R.A., Perrone, C.E., Orentreich, N., Cefalu, W.T., and Gettys, T.W. (2011). Dietary methionine restriction increases fat oxidation in obese adults with metabolic syndrome. J. Clin. Endocrinol. Metab. *96*, E836–E840.

Plaisance, E.P., Henagan, T.M., Echlin, H., Boudreau, A., Hill, K.L., Lenard, N.R., Hasek, B.E., Orentreich, N., and Gettys, T.W. (2010). Role of ß-adrenergic receptors in the hyperphagic and hypermetabolic responses to dietary methionine restriction. Am. J. Physiol. Regul. Integr. Comp. Physiol. *299*, R740–R750.

Reiner, A., Yekutieli, D., and Benjamini, Y. (2003). Identifying differentially expressed genes using false discovery rate controlling procedures. Bioinformatics *19*, 368–375.

Richie, J.P., Jr., Leutzinger, Y., Parthasarathy, S., Malloy, V., Orentreich, N., and Zimmerman, J.A. (1994). Methionine restriction increases blood glutathione and longevity in F344 rats. FASEB J. *8*, 1302–1307.

Rooney, J., Oshida, K., Vasani, N., Vallanat, B., Ryan, N., Chorley, B.N., Wang, X.T., Bell, D.A., Wu, K.C., Aleksunes, L.M., et al. (2018). Activation of Nrf2 in the liver is associated with stress resistance mediated by suppression of the growth hormone-regulated STAT5b transcription factor. PLoS One *13*, e0200004.

Slump, P., and Schreuder, H.A. (1973). Oxidation of methionine and cystine in foods treated with hydrogen peroxide. J. Sci. Food Agric. *24*, 657–661.

Stone, K.P., Ghosh, S., Kovalik, J.P., Orgeron, M., Wanders, D., Sims, L.C., and Gettys, T.W. (2021). The acute transcriptional responses to dietary methionine restriction are triggered by inhibition of ternary complex formation and linked to Erk1/2, mTOR, and ATF4. Sci. Rep. *11*, 3765.

Stone, K.P., Wanders, D., Orgeron, M., Cortez, C.C., and Gettys, T.W. (2014). Mechanisms of increased in vivo insulin sensitivity by dietary methionine restriction in mice. Diabetes *63*, 3721–3733.

Subramanian, A., Tamayo, P., Mootha, V.K., Mukherjee, S., Ebert, B.L., Gillette, M.A., Paulovich, A., Pomeroy, S.L., Golub, T.R., Lander, E.S., et al. (2005). Gene set enrichment analysis: a

knowledge-based approach for interpreting genome-wide expression profiles. Proc. Natl. Acad. Sci. U S A *102*, 15545–15550.

Sun, L., Sadighi Akha, A.A., Miller, R.A., and Harper, J.M. (2009). Life-span extension in mice by preweaning food restriction and by methionine restriction in middle age. J. Gerontol. A Biol. Sci. Med. Sci. *64*, 711–722.

Vluggens, A., Andreoletti, P., Viswakarma, N., Jia, Y., Matsumoto, K., Kulik, W., Khan, M., Huang, J., Guo, D., Yu, S., et al. (2010). Reversal of mouse Acyl-CoA oxidase 1 (ACOX1) null phenotype by human ACOX1b isoform [corrected]. Lab. Invest *90*, 696–708.

Wanders, D., Burk, D.H., Cortez, C.C., Van, N.T., Stone, K.P., Baker, M., Mendoza, T., Mynatt, R.L., and Gettys, T.W. (2015). UCP1 is an essential mediator of the effects of methionine restriction on energy balance but not insulin sensitivity. FASEB J. *29*, 2603–2615.

Wanders, D., Forney, L.A., Stone, K.P., Burk, D.H., Pierse, A., and Gettys, T.W. (2017). FGF21 mediates the thermogenic and insulin-sensitizing effects of dietary methionine restriction but not its effects on hepatic lipid metabolism. Diabetes *66*, 858–867.

Wanders, D., Ghosh, S., Stone, K.P., Van, N.T., and Gettys, T.W. (2014). Transcriptional impact of dietary methionine restriction on systemic inflammation: relevance to biomarkers of metabolic disease during aging. Biofactors *40*, 13–26.

Wanders, D., Stone, K.P., Forney, L.A., Cortez, C.C., Dille, K.N., Simon, J., Xu, M., Hotard, E.C., Nikonorova, I.A., Pettit, A.P., et al. (2016). Role of GCN2-independent signaling through a non-canonical PERK/NRF2 pathway in the physiological responses to dietary methionine restriction. Diabetes *65*, 1499–1510.

Zimmerman, J.A., Malloy, V., Krajcik, R., and Orentreich, N. (2003). Nutritional control of aging. Exp. Gerontol. *38*, 47–52.

STAR★METHODS

KEY RESOURCES TABLE

REAGENT or RESOURCE	SOURCE	IDENTIFIER
Antibodies		
SCD1 (E-15) Antibody	Santa Cruz Biotechnology	Cat# sc-14720; RRID:AB_2183121
Fatty Acid Synthase (G-11) Antibody	Santa Cruz Biotechnology	Cat# sc-48357;, RRID:AB_627584
Acetyl-CoA Carboxylase Antibody	Cell Signaling Technology	Cat# 3662;, RRID:AB_2219400
Anti-Uncoupling Protein 1 Antibody	Millipore	Cat# AB1426;, RRID:AB_2213784
PDC-E2 (B-2) Antibody	Santa Cruz Biotechnology	Cat# sc-271534;, RRID:AB_10649809
Anti-β-Actin Antibody	Sigma-Aldrich	Cat# A5441, RRID:AB_476744
Deposited data		
Liver and IWAT RNAseq	NCBI GEO	Accession number: GSE162918 (Liver), GSE162917 (IWAT)
Experimental models: organisms/strains		
C57BL/6J	Jackson Laboratory	Cat# JAX:000664;, RRID:IMSR_JAX:000664
Software and algorithms		
JMP Pro 14	JMP Software	RRID:SCR_014242
GraphPad Prism 8	GraphPad Software	RRID:SCR_002798
Ingenuity Pathway Analysis	QIAGEN	RRID:SCR_008653
GSEA v4.1.0 for Windows	Subramanian et al., 2005	RRID:SCR_003199
DESeq2 Software	Love et al., 2014	RRID:SCR_015687
R Project for Statistical Computing	R Core Team (2013). R: A language and environment for statistical computing. R Foundation for Statistical Computing, Vienna, Austria. URL http://www.R-project.org/	RRID:SCR_001905

RESOURCE AVAILABILITY

Lead contact

Further information and requests for resources and reagents should be directed to and will be fulfilled by the lead contact, Thomas W. Gettys (Thomas.gettys@pbrc.edu).

Materials availability

The study did not generate new unique reagents. The expression profiling data has been deposited in NCBI under GEO accession numbers (Liver: GSE162918, IWAT: GSE162917).

Data and code availability

All data generated or analyzed during this study will be available from the lead contact upon request.

EXPERIMENTAL MODEL AND SUBJECT DETAILS

Formulation of elemental control and MR diets

All experiments were reviewed and approved by the Pennington Institutional Animal Care and Use Committee using guidelines established by the National Research Council, the Animal Welfare Act, and the Public Health Service Policy on the humane care and use of animals. Pelleted diets (Dyets Inc., Bethlehem, Pennsylvania) containing either 0.86% methionine (Con) and no cysteine or 0.17% methionine (MR) and no cysteine were provided *ad libitum* to the mice. The diets were isocaloric at 15.96 kJ/g, with 18.9% of energy from fat (corn oil), 64.9% from carbohydrate, and 14.8% from a custom mixture of L-amino acids. The details of amino acid content and other macronutrients in the diet are provided in Table 1.

Production of control and oxidized casein for diet formulation

Casein was isolated from a mixture of skim milk and water (1:2) by lowering the pH to 4.6 with 1.0 M HCl, followed by centrifugation at 8000 rpm for 30 minutes. The supernatant containing the sugars was collected and discarded, and the pelleted casein was washed with an equal volume of deionized water prior to repeating the centrifugation step. This washing and centrifugation step was repeated a total of three times. The pelleted casein was then divided into two lots. Lot 1 was lyophilized and retained for use in formulation of the casein control diet. Lot 2 was re-suspended in deionized water, adjusted to pH 2.5, and hydrogen peroxide was added to a final concentration of 10%. The suspension was incubated under a fume hood on a heated stir plate for 1 h at 90°C. Hydrogen peroxide was then removed by suction filtration through a sieve with three volumes of deionized water, and the casein was lyophilized and used to formulate the oxidized casein MR diet. The control casein and the oxidized casein were submitted to Covance Inc. (Princeton, NJ) for amino acid analysis (see Figures 1A and 1B) prior to formulation of the respective casein control and oxidized casein MR diets by Dyets Inc. as follows (Bethlehem, PA).

Formulation of oxidized Casein MR and Casein control diets

The casein control and oxidized MR diets were formulated to match the 14% nitrogen content of the Ele Con and Ele MR diets. The protein content of the control casein was 88.8 g/100 g protein, and the oxidized casein was 80.1 g/100 g protein, necessitating the addition of 141 g of control casein per kg of Cas CON diet and 153 g of oxidized casein per kg of Ox Cas MR diet to account for differences in moisture content between the two lots of casein (Table 2). The amino acid content of the respective proteins is shown in Figures 5A and 5B, illustrating that the oxidation procedure reduced the concentrations of lysine, methionine, cysteine, and tryptophan in the oxidized casein and left all other amino acids essentially unchanged. To correct these differentials and adjust the methionine concentrations to produce the Con Cas and Ox Cas MR diets, the following additions were made during diet formulation. Based on the methionine content of the control casein, this produced a concentration of 3.58 g of methionine per kg of Cas Con diet, so 5.02 g of methionine was added to bring the final concentration to 8.6 g methionine per kg diet (e.g., 0.86%) (Table 2). Based on the lysine content of the control casein, 7.57 g of additional lysine was added to bring the final concentration of lysine to 18 g/kg Cas Con diet (e.g., 1.8%) to match the lysine content of the Ele CON diet (Tables 2 and 1). Based on the reduction of methionine in the oxidized casein, this produced a concentration of 0.23 g/kg Ox Cas MR diet, so 1.47 of methionine was added to bring the final concentration to 1.7 g methionine per kg diet (e.g., 0.17%) (Table 2). Based on the reduction of lysine content of the oxidized casein, 11.19 g of lysine was added to match the lysine content of the Cas Con and Ele Con diets (Tables 2 and 1). And based on the reduction of tryptophan content of the oxidized casein, 1.515 g of tryptophan was added to match the tryptophan content of the Cas Con and Ele Con diets (Tables 2 and 1). The final energy content of Cas Con and Ox Cas MR diets was 16.0 kJ/g (Table 2). The method is described under Patent 10897921 (Finley et al., 2021).

Experimental animal protocol and metabolic phenotyping

Male C57Bl/6J mice were purchased from Jackson Labs (Bar Harbor, ME) at 5 weeks of age and housed individually in plastic cages on corncob bedding with micro-isolator tops. Sentinel mice were co-housed with the experimental mice and screened for mouse pathogens at regular intervals. Half of the 40 mice were adapted to the Ele Con diet for 2 weeks, whereas the other half were adapted to the Cas Con diet for 2 weeks. Thereafter, half the mice on each Con diet were randomly assigned to receive either the Ele MR diet or Ox Cas MR diet. Food intake and water consumption were evaluated at weekly intervals thereafter for the 8-week duration of the study. Food consumption was measured by weighing the food provided at the beginning of the measurement period and subtracting the remaining food at the end of the feeding period. Wasted food was collected and weighed by sifting the corncob bedding over wire mesh. Water consumption was measured in a similar manner. Food and water were provided *ad libitum* to all groups. Animals were housed at 23°C for the entire study and maintained on a 12-h light/dark cycle. Body weight and composition were also measured at weekly intervals via nuclear magnetic resonance spectroscopy (NMR; Bruker Mini Spec, Billerica, MA).

METHOD DETAILS

Indirect calorimetry

After 8 weeks on the prescribed diet, animals were transferred to the Animal Metabolism and Behavior Core Facility at Pennington Biomedical Research Center for measurement of activity and energy

expenditure using a Comprehensive Laboratory Animal Monitoring System (CLAMS System; Columbus Instruments, Columbus, OH). Mice were allowed to acclimate to the metabolic chambers for a period of 12 h prior to initiation of data collection. Oxygen consumption and carbon dioxide production was evaluated for each animal at 40 minute intervals over a period of 72 h. Energy expenditure (EE) was calculated as VO2*(2.815+(1.232*RQ))*4.187, where RQ is the ratio of VCO2 produced to VO2 consumed. Voluntary activity was monitored while animals remained in the chambers using an OPTO-M3 sensor system. Body composition was measured via NMR both immediately prior to and upon completion of EE analysis and extrapolated over the period of EE measurements. Following the measurement of EE, mice were returned to their home cages and continued on their respective diets.

Insulin tolerance testing and tissue harvest

After a 4-day re-adaption period after indirect calorimetry, animals were subjected to insulin tolerance testing. Mice were fasted for a period of 4 h prior to testing. Insulin was provided via intraperitoneal injections (Humulin-R, 50 U/kg body weight), and blood was tested on a One Touch blood glucometer via tail nick at baseline, and 15, 30, 45, and 60 minutes after insulin. Upon completion, mice were returned to their home cages and allowed to re-equilibrate for 1 week prior to being euthanized via CO2-inhalation followed by decapitation for collection of trunk blood. Animals were fasted 4 h prior to being euthanized. Inguinal white adipose tissue (IWAT), brown adipose tissue (BAT), and liver were harvested and immediately snap frozen in liquid nitrogen and placed at −80°C until analysis. Blood was allowed to clot at room temperature for 30 minutes, and serum was obtained from clotted blood after centrifugation and stored at −80°C.

Triglyceride assay and serum hormones

Hepatic and serum triglyceride content was determined using a colorimetric assay (Cayman Chemicals; Ann Arbor, MI). Fasting serum insulin and FGF21 concentrations were determined via enzyme-linked immunosorbent assays (ELISA), according to the manufacturer's protocols (insulin—Millipore, Billerica, MA; FGF21—R&D Systems, Minneapolis, MN).

Western blotting

Whole-cell lysates of liver, IWAT, and BAT were prepared by homogenizing tissue in buffer (150 mM sodium chloride, 1 mM EDTA, 1 mM EGTA, 10 mM Tris, 1% Triton X-100, 0.5% NP-40), and protein was quantitated by Lowry assay. Fifty microgram of whole-cell extracts was used for liver SCD1, 35 μg for liver FAS, 30 μg for liver ACC and IWAT UCP1, and 3 μg for BAT UCP1. Proteins were separated by sodium dodecyl sulfate–polyacrylamide gel electrophoresis and transferred to polyvinylidene fluoride membranes. Expression of liver SCD1, FAS, ACC, and IWAT UCP1 were detected and standardized to β-actin (Sigma Millipore, St. Louis, MO; A-5441). The FASN (sc-48357) and SCD-1 (sc-14720; E-15) antibodies were from Santa Cruz Biotechnology (Dallas, TX), whereas the ACC antibody (#3662) was from Cell Signaling (Danvers, MA). PDC-E2 (sc-271534) was used as loading control for BAT UCP1 as described previously (Wanders et al., 2015).

RNA isolation and RNAseq

Total RNA was isolated from IWAT and livers using RNeasy Mini kit (Qiagen, Valencia, CA). RNA concentrations were measured using Nanodrop ND-1000 spectrophotometer (Nanodrop Technologies, Wilmington, DE). Total RNA was analyzed using the Agilent Bioanalyzer RNA 1000 chip as a QC step to determine the quality of the RNA. Samples were verified to have RIN values of >7, indicating high-quality RNA. Samples were then processed for library construction using the Lexogen Quant-Seq 3′ mRNA-Seq Library Prep Kit. Completed libraries were analyzed on the Agilent Bioanalyzer High Sensitivity DNA chip to verify correct library size. All libraries were pooled in equimolar amounts and sequenced on the Illumina NextSeq 500 at 50bp forward read and 6bp forward index read. Primary data analysis was performed using the Lexogen Quantseq pipeline V1.8.8 on the Bluebee platform for quality control, mapping, and read count tables. The gene expression profiles were assessed from six replicates for each tissue for each dietary group. CLC Genomics Workbench was used to process data. The expression profiling data have been deposited in NCBI under GEO accession numbers (Liver: GSE162918, IWAT: GSE162917).

Prior to differential gene expression analysis, scaled normalized count data for samples from the four treatment groups (Ele CON, Ele MR, Cas CON, and Ox Cas MR) were analyzed via principal components analysis (PCA) (using *prcomp* package in R, http://www.R-project.org/) to cluster samples based on gene

expression similarities and to identify potential outliers. After removal of outlier samples, differential analysis of RNA read count data was performed using DESeq2 software (Love et al., 2014), which models read counts as a negative binomial distribution and uses an empirical Bayes shrinkage-based method to estimate signal dispersion and fold-changes. Gene expression signals were logarithmically transformed (to base 2) for all downstream analyses (the lowest expression value being set to 1 for this purpose). Genes with an absolute log fold-change ≥ 1 and false discovery rate (FDR) of 5% were considered as differentially expressed.

Preranked GSEA analysis

For both IWAT and liver RNAseq datasets, enrichment analysis of biological pathways (gene sets) was conducted via gene set enrichment analysis (GSEA) (Subramanian et al., 2005). Specifically, the GSEA-preranked option was used and enrichment computed by first ranking all genes based on their log fold-changes in the respective comparisons. Enrichment was computed either on user-defined custom pathways or pathways present in the Kyoto Encyclopedia of Genes and Genomes (KEGG) database (Ogata et al., 1999) available from the Molecular Signatures Database repository (MSigDb, http://software.broadinstitute.org/gsea/msigdb/, (Liberzon et al., 2015)). Statistical significance for the observed enrichment was ascertained by permutation testing over size-matched gene-sets. Gene-sets with FDR$\leq$5% were considered as significantly enriched (Reiner et al., 2003). The individual contributions of pathway genes to the pathway enrichment signal were visualized via enrichment plots depicting the trajectory of a normalized pathway enrichment score against the rank of the pathway genes in the context of the full gene list.

Ingenuity pathway analysis (IPA)

Pathway over-representation analysis was conducted using IPA (QIAGEN Inc., https://www.qiagenbioinformatics.com/products/ingenuity-pathway-analysis), considering 2,437 differentially expressed genes from the Ele MR to Ele CON liver samples, 3,273 differentially expressed genes from the Ox Cas MR to Cas CON liver samples, 1,637 differentially expressed genes from the Ele MR to Ele CON IWAT samples, and 2,041 differentially expressed genes from the Ox Cas MR to Cas CON IWAT samples (absolute log fold-change $\geq$1.3, FDR$\geq$0.3). Within IPA, the Upstream Regulator Analysis module was utilized to identify putative gene regulators responsible for the observed transcriptional patterns produced by the Ele MR diet compared with the Ox Cas MR diet in the two tissues. Several possible types of upstream regulators were considered including transcription factors, cytokine receptors, G-protein-coupled receptors, ligand-dependent nuclear receptors, and translation regulators. Differential regulation of canonical pathways across the two diets and tissues were also examined. Regulators and canonical pathways with an activation z-score $\geq$ 2 or $\leq$ 2 were considered to be activated or inhibited respectively. Heat maps were used to visualize differential or common upstream regulators and canonical pathways affected by the Ele MR compared with the Ox Cas MR diet.

qPCR analysis

Quantitative PCR analysis of IWAT and liver mRNA expression of known MR target genes was performed after reverse transcription of 2µg RNA into cDNA. Gene expression was measured using 10ng cDNA and SYBR (Biorad). Data were normalized to cyclophilin expression and expressed as fold-change relative to the Ele Con group in each tissue. Primer sequences are provided in Table S1.

Metabolomics analysis

Frozen liver (30–50 mg) was powdered in liquid nitrogen and submitted to the Mass Spectrometry Core at UT Knoxville for non-targeted metabolomics (https://chem.utk.edu/facilities/biological-and-small-molecule-mass-spectrometry-core-bsmmsc/). Data were normalized to sample weight, and relative quantities of sulfur amino acid metabolites were compared between Ele Con, Ele MR, Cas Con, and Ox Cas MR-fed groups.

QUANTITATIVE AND STATISTICAL ANALYSIS

The body weight and food intake over time was analyzed as a repeated measure, one-way analysis of variance (ANOVA), with group means at each time compared using the variance associated with diet x time point as the error term. Group differences in body composition, energy expenditure, endocrine and metabolite measures, and gene expression measures were compared using a one-way ANOVA, and the

significance of diet effects was tested using residual variance as the error term. Least squares means ± SEM are plotted and annotated to denote significant differences. Group differences in energy expenditure were compared using analysis of covariance (ANCOVA) as previously described (Forney et al., 2020). Least squares means were calculated for each dietary group during the day and night after accounting for variation in EE attributable to differences in lean mass, fat mass, and activity among the mice. The ANCOVA was conducted using JMP Discovery software (Cary, NC), and the ANOVA was conducted using GraphPad Prism (GraphPad Software; San Diego, CA). Protection against type I errors was set at 5% ($P<0.05$).